

Peculiar Motions Of Clusters In The Perseus–Pisces Region

R.J. Smith¹, M.J. Hudson^{1,2}, J.R. Lucey¹ and J. Steel¹

¹ Department of Physics, University of Durham, South Road, Durham DH1 3LE, U.K.

² Department of Physics and Astronomy, University of Victoria, P.O. Box 3055, Victoria BC V8W 3PN, Canada

Abstract. We present results of a new study of peculiar motions of 7 clusters in the Perseus–Pisces (PP) region, using the Fundamental Plane as a distance indicator. The sample is calibrated by reference to 9 additional clusters with data from the literature. Careful attention is paid to the matching of spectroscopic and photometric data from several sources.

For six clusters in the PP supercluster no significant peculiar motions are detected. For these clusters we derive a bulk motion of $60 \pm 220 \text{ km s}^{-1}$, in the CMB frame, directed towards the Local Group. This non-detection is in marginal conflict with previous Tully–Fisher studies. Two clusters in the background of the supercluster exhibit significant negative peculiar velocities, characteristic of backside infall into PP.

A bulk-flow fit to all 16 clusters reveals a statistically insignificant motion of $430 \pm 280 \text{ km s}^{-1}$ towards $l = 265^\circ, b = 26^\circ$ (CMB frame). Comparison with the velocity field predicted from the IRAS 1.2Jy survey yields $\beta = 1.0 \pm 0.5$. We find no evidence for residual bulk motions generated by mass concentrations beyond the limiting depth of the IRAS density field.

1 Introduction

The Perseus–Pisces (PP) supercluster, at $cz \sim 5000 \text{ km s}^{-1}$, lies directly opposite the apex of the large-scale streaming detected by Lynden-Bell et al. (1988). If, as in the flow model of Faber & Burstein (1988), the local dynamics are dominated by a single ‘Great Attractor’ (GA) beyond Hydra–Centaurus, then the peculiar velocity at PP is predicted to be $\lesssim 150 \text{ km s}^{-1}$. If however, very distant sources are responsible for large-scale motions, then the PP region would be expected to share in a bulk streaming velocity of $\sim 500 \text{ km s}^{-1}$.

Measurements of bulk motion in PP have been made by Willick (1991) and by Han & Mould (1992). These studies, employing the Tully–Fisher (TF) relation for spiral galaxies, both argue for a large bulk motion ($\sim 400 \text{ km s}^{-1}$). Courteau et al. (1993) support this result, and invoke very large-scale density fluctuations to account for the large coherence length of the flow.

Motions in the PP region have not been well-studied using elliptical galaxy distance indicators. Here, we describe a programme to measure peculiar motions for 7 clusters in PP, using the Fundamental Plane (FP) relation for early-type galaxies. Spectroscopic and photometric data and methods are presented in full by Smith et al. (1997a). Hudson et al. (1997) present a detailed account of the FP fits and velocity field analyses.

2 A new survey

The current survey is based on a sample of early-type galaxies in clusters. Clusters are chosen since *a priori* grouping in redshift-space reduces the magnitude of Malmquist bias effects. This is especially desirable in regions of high density contrast, such as PP, where corrections for inhomogeneous Malmquist bias would otherwise be large and uncertain. Early-type galaxies provide the best means of probing cluster cores with minimal contamination from field galaxies.

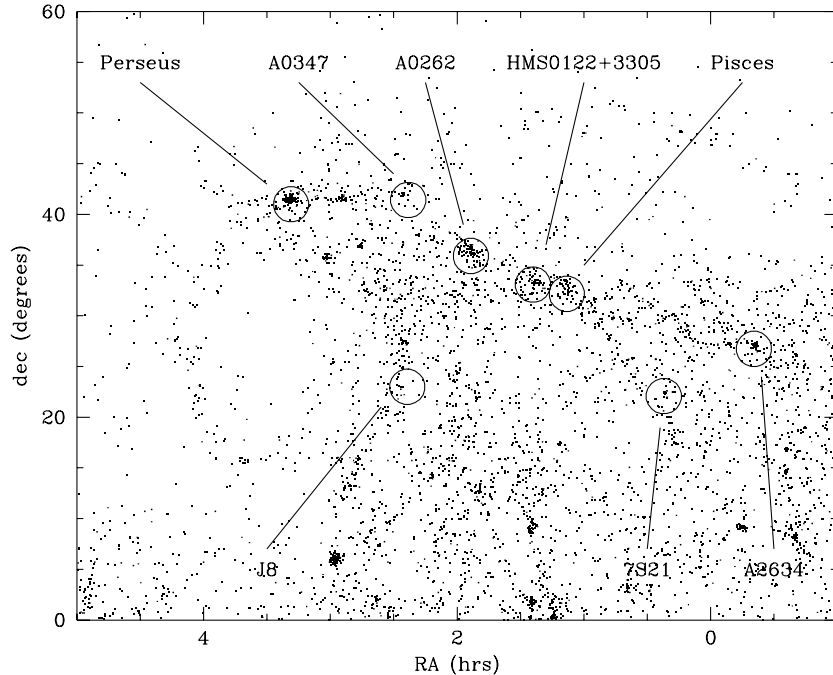


Fig. 1. Projected distribution of $cz < 12000 \text{ km s}^{-1}$ galaxies in the PP region, selected from the ZCAT compilation of Huchra et al. (1993). Open circles mark the location of clusters observed in this programme.

Figure 1 shows the projected distribution of the cluster sample, along with the projected galaxy distribution. The supercluster ‘ridge’ at $cz \sim 5000 \text{ km s}^{-1}$

is evident in the plot, and is traced by six observed clusters (Perseus, A0347, A0262, HMS0122+3305, Pisces and 7S21). The sample includes the cluster J8, located in the background of the ridge, at $cz \sim 9000 \text{ km s}^{-1}$. The cluster A2634 is formally part of our calibration sample, but can also be considered as a PP background cluster.

2.1 Photometry

The fundamental plane parameters R_e and $\langle \mu \rangle_e$ are measured from R-band photometric observations obtained at the 1m Jacobus Kapteyn Telescope on La Palma. Standard reduction techniques are applied, with parameters finally being derived from an $R^{1/4}$ -law fit to the aperture magnitude growth-curve. Internal and external comparisons indicate that measurement uncertainties in the photometric parameters contribute distance errors smaller than 1.5% per galaxy.

2.2 Spectroscopy

Velocity dispersions, σ , are derived from spectra obtained at the 2.5m Isaac Newton Telescope on La Palma. Internal comparisons indicate an average uncertainty of 7.6% per measurement. The aperture correction of Jørgensen, Franx & Kjærgaard (1995b) is adopted, with all σ measurements referred to a physical aperture of diameter $1.19 h^{-1} \text{ kpc}$.

In order to construct large samples of peculiar velocity data, it is necessary to merge measurements from different observing runs, instrumental configurations, observers, etc. Despite careful attempts to correct for aperture effects, systematic offsets often persist at the 3-4% level between velocity dispersions measured on different systems. Whilst the precise cause of these offsets is not fully understood, it is vital that they are corrected for and (most importantly) that the uncertainties on these corrections are included in the overall error budget.

The removal of systematic offsets can be achieved by intercomparison of measurements for galaxies common to two or more systems. The set of overlap observations used here includes 1300 measurements for 350 different galaxies, on 19 systems. We adopt the (aperture-corrected) Lick system of Davies et al. (1987) as our ‘standard system’. For all other systems, we determine corrections required to match onto this standard. Since many galaxies have data on more than two systems, the fit has been performed simultaneously for all the corrections.

From bootstrap realisations of this process, we estimate the error on each system correction and also the correlation between the errors for different systems. The mean systematic error in σ can then be computed for each cluster. For the PP ridge clusters, this ‘system matching’ error is $\sim 100 \text{ km s}^{-1}$.

2.3 Fundamental Plane fits

Since the PP cluster sample studied here has very limited sky coverage, it would be impossible, given the present data alone, to differentiate between a bulk motion of PP and a velocity zero-point error. In order to resolve this degeneracy,

we utilise data for a well-distributed sample of ‘calibration clusters’. Specifically, we include six rich clusters (A0194, A0539, A3381, A3574, DC2345-28, Hydra) from the work of Jørgensen, Franx & Kjærgaard (1996), and three well-studied clusters (Coma, A2199, A2634) from Lucey et al. (1997). Photometric parameters from the three sources can be brought onto a consistent system by the application of well defined offsets (Smith et al. 1997a).

Using the resulting sample of 16 clusters, we fit simultaneously for the global FP slope parameters, and for the individual cluster zero-points. The fit is performed by minimizing residuals in $\log \sigma$. This ‘inverse fit’ is unbiased by selection on photometric parameters (radius, surface brightness or any combination thereof, such as total magnitude). The inverse fit would, however, be biased by any explicit selection on $\log \sigma$. In the present work, no such selection occurs, since galaxies are not thrown out of the sample, *a posteriori*, based on their measured velocity dispersions.

The best fitting fundamental plane for the sample is given by

$$\log R_e = 1.383(\pm 0.040) \log \sigma + 0.326(\pm 0.011) \langle \mu \rangle_e + \gamma_{\text{cl}}$$

with scatter equivalent to a distance error of 20% per galaxy. The cluster zero-points, γ_{cl} , are used to derive relative distances, as discussed below. In practice we find that an initial calibration, based on the assumption of zero peculiar motion for Coma, leads to a mean radial peculiar velocity for the sample which is indistinguishable from zero. Hereafter, we adopt this simply-defined zero-point for the present analysis.

In Figures 2 and 3 we show the FP fits for the 16 clusters separately. The slopes derived for individual clusters are consistent in every case with the slope of the globally-defined FP.

3 Results

3.1 Peculiar velocities

Distances and peculiar velocities for the 16 cluster sample are presented in Table 1. Here, the distance estimates have been corrected for homogeneous Malmquist bias. The use of a cluster sample leads to corrections of only 0.5–2% for this effect. Inhomogeneous Malmquist bias corrections are expected to be smaller than this, and are neglected here. The velocity vectors for clusters in PP are shown in graphical form in Figure 4.

The present data do not indicate a significant peculiar motion for any of the six clusters in the ridge of PP. In the background of the supercluster, J8 and A2634 display large, significant peculiar velocities in the sense expected if they are involved in ‘backside infall’ into PP.

In Table 2, we present comparisons between the current results and peculiar velocities measured by other authors. The agreement is good for most clusters.

Table 1. Cluster distances and peculiar velocities. Column 3 indicates the source of photometric and spectroscopic data, in that order. For each cluster, N_{gal} indicates the number of galaxies used in the fit. Distances and peculiar velocities (in the CMB frame) are given in km s^{-1} . The velocity error is a 1σ random error including a contribution from uncertainty in the cluster redshift.

	Cluster	Data Source	N_{gal}	Distance	Peculiar Velocity	Velocity error
PP ridge	7S21	1,1	7	5448	69	450
	Pisces	1,1	25	4583	131	208
	HMS0122	1,1	9	4680	−44	352
	A0262	1,1	10	4787	−259	340
	A0347	1,1	8	5590	−277	430
	Perseus	1,1	31	5176	−136	307
PP background	J8	1,1	13	10449	−1032	602
	A2634	2,2	35	10111	−960	364
Calibrators	A2199	2,2	36	9285	−342	325
	Coma	2,2	71	7200	0	204
	A0194	3,4+5	19	4379	743	230
	A0539	3,4	22	8380	234	402
	A3381	3,4	14	10883	578	593
	A3574	3,4	7	4217	655	369
	DC2345-28	3,5	27	8645	−174	362
	Hydra	3,4+5	18	3946	30	239

References for data sources: 1 – Smith et al. (1997a); 2 – Lucey et al. (1997); 3 – Jørgensen, Franx & Kjærgaard (1995a); 4 – Jørgensen, Franx & Kjærgaard (1995b); 5 – Lucey & Carter (1988).

3.2 Bulk flow fits

As a simple description of the local velocity field, we consider a bulk flow model with three free parameters. Fitting for all 16 clusters, we find a bulk velocity of $430 \pm 198 \text{ km s}^{-1}$, in the CMB frame, directed towards $l = 264.6^\circ, b = -25.6^\circ$. Uncertainties in the matching of spectroscopic systems raise the total error on the bulk-flow amplitude to 280 km s^{-1} . The bulk motion of this sample of clusters is therefore not statistically significant.

Fitting a bulk-flow model for only the six PP ridge clusters, no streaming motion of the supercluster is detected. The fit yields a PP bulk-flow of $59 \pm 221 \text{ km s}^{-1}$ (toward the Local Group). The quoted error, includes system matching uncertainties and a contribution from the uncertainty in setting a velocity zero-point for the sample.

Table 2. Comparisons of present results with peculiar velocities measured from the TF relation by Han & Mould (1992), and from the FP by Baggley (1996) and Scoddeggio et al. (1997). Baggley’s results are based on a subset of the EFAR data. Note that our ‘Pisces’ cluster is the ‘N507 group’ of Scoddeggio et al.

Cluster	This study	Han & Mould (TF)	Baggley (FP)	Scoddeggio (FP)
Pisces	131 ± 208	76 ± 296		420 ± 238
HMS0122	-44 ± 352	311 ± 374		
A0262	-259 ± 340	-576 ± 391	782 ± 429	-157 ± 203
A2634	-960 ± 364	-906 ± 639	-978 ± 967	-308 ± 336
A2199	-342 ± 325		697 ± 497	
Coma	(0 ± 204)	80 ± 428	(0 ± 356)	42 ± 196
A0539	234 ± 402	11 ± 621		
DC2345-28	-174 ± 362		591 ± 403	
Hydra	30 ± 239	184 ± 296		

3.3 Comparison with the predicted velocity field

A more realistic model of the flow field can be obtained by predicting the peculiar velocity of each cluster from a suitable redshift survey, with $\beta = \Omega^{0.6}/b$ as a single free parameter. Here we employ the IRAS 1.2 Jy survey, within 12000 km s^{-1} , the IRAS density field being kindly provided to us by M. Strauss.

The best fit to the observed cluster velocities is obtained for $\beta = 0.94 \pm 0.48$. While this represents a marginal detection of β , the errors are too large for useful constraints to be derived from the present sample.

After subtraction of the IRAS-predicted peculiar velocities from the observed motions, the residual (CMB frame) bulk motion of the sample is $383 \pm 294 \text{ km s}^{-1}$, directed towards $l = 313.2^\circ, b = -26.4^\circ$. We conclude from this non-detection, that mass concentrations beyond 12000 km s^{-1} are not required to explain the observed velocities.

4 Conclusions

We have completed a new survey of cluster motions in the PP region, using the FP as a distance indicator. Careful attention has been paid to the construction of a homogeneous, merged dataset, and to accounting for systematic uncertainties in this procedure.

We derive an insignificant bulk motion ($-60 \pm 220 \text{ km s}^{-1}$ towards the Local Group) for 6 clusters in the main ridge of the supercluster. This result is in marginal conflict with Tully–Fisher surveys by Willick (1991), Han & Mould (1992) and Courteau et al. (1993). Two clusters in the background of PP show evidence for ‘backside infall’ into the supercluster.

Comparing the observed cluster motions with the velocity field predicted from the IRAS 1.2Jy survey, we find a best fit for $\beta = 1.0 \pm 0.5$. There is no

evidence for residual bulk flows generated by sources beyond the IRAS density field limit.

A new, all-sky, survey of ~ 50 Abell clusters within 12000 km s^{-1} is currently in progress (see Smith et al. 1997b, this volume). This improved sample, will yield useful constraints on β , in addition to a reliable measurement of the bulk motion.

References

Aaronson, M., Bothun, G., Mould, J.R., Huchra, J.P., Schommer, R., Cornell, M. 1986, ApJ, 302, 536

Baggley, G., 1996, PhD thesis, University of Oxford

Courteau, S., Faber, S.M., Dressler, A., Willick, J.A. 1993, ApJ, 412, L51

Davies, R.L., Burstein, D., Dressler, A., Faber, S.M., Lynden-Bell, D., Terlevich, R.J., Wegner, G. 1987, ApJS, 64, 581

Faber, S.M., Burstein, D. 1988, in Coyne, G., Rubin, V.C., eds, Proceedings of the Vatican Study Week, Large Scale Motions in the Universe. Princeton Univ. Press, Princeton, p. 135

Han, M.S., Mould, J.R. 1992, ApJ, 396, 453

Huchra, J.P., Geller, M.J., Clemens, C.M., Tokarz, S.P., Michel, A. 1993, Astronomical Data Center archives

Hudson, M.J., Lucey, J.R., Smith, R.J., Steel, J. 1997, MNRAS, submitted

Jørgensen, I., Franx, M., Kjærgaard, P. 1995a MNRAS, 273, 1097

Jørgensen, I., Franx, M., Kjærgaard, P. 1995b MNRAS, 276, 1341

Jørgensen, I., Franx, M., Kjærgaard, P. 1996 MNRAS, 280, 167

Lucey, J.R., Carter, D. 1988, MNRAS, 235, 1177

Lucey, J.R., Guzmán, R., Steel, J., Carter, D. 1997, MNRAS, submitted

Lynden-Bell, D., Faber, S.M., Burstein, D., Davies, R.L., Dressler, A., Terlevich, R.J., Wegner, G. 1988, ApJ, 326, 19

Scodéglio, M. et al. 1996, this volume

Smith, R.J., Lucey, J.R., Hudson, M.J., Steel, J. 1997a, MNRAS, submitted

Smith, R.J., Hudson, M.J., Lucey, J.R., Schlegel, D.J., Davies, R.L., Baggley, G. 1997b, this volume

Willick, J.A. 1991, ApJ, 351, L51

FP

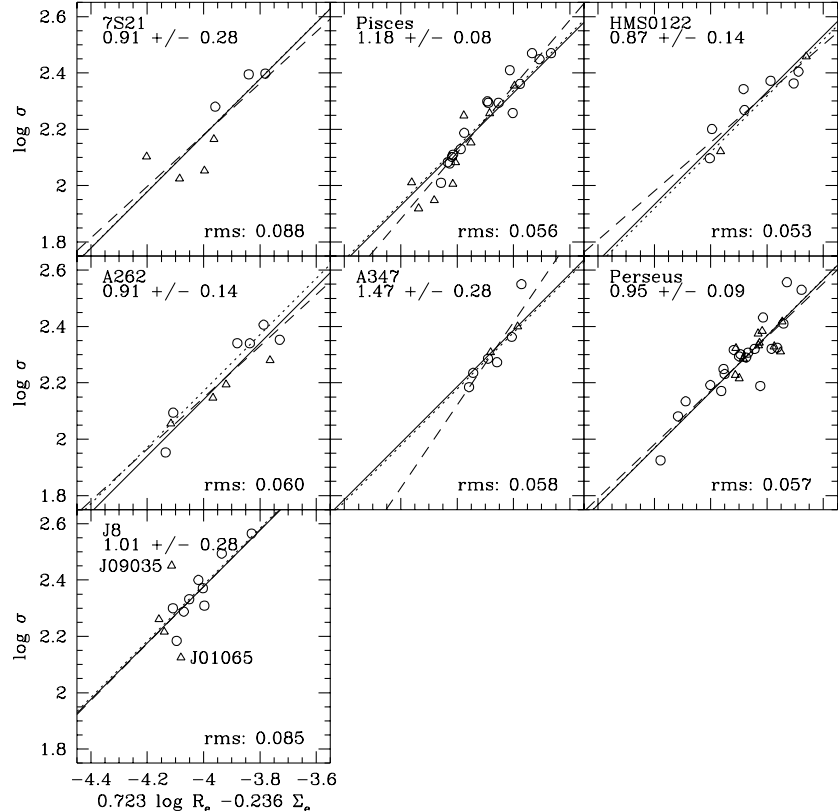


Fig. 2. FP data and fits for the clusters 7S21, Pisces, HMS0122, A0262, A0347, Perseus and J8. Early type galaxies (E, E/S0, D or cD) are indicated by circles, later types by triangles. The solid line shows the global inverse FP, found by minimising σ residuals simultaneously over the whole cluster sample with the same slope but varying zero-points for each cluster. Each cluster's measured scatter in σ around this global fit is given in the lower right-hand corner. Galaxies which deviate from the global fit by more than 2.5 times the global scatter are labelled. The dotted line shows the median of the residuals with the slope fixed from the whole cluster sample. The dashed line shows the best slope and zero-point fit to the individual cluster. The individual cluster slope relative to the global slope is given in the upper left-hand corner.

FP

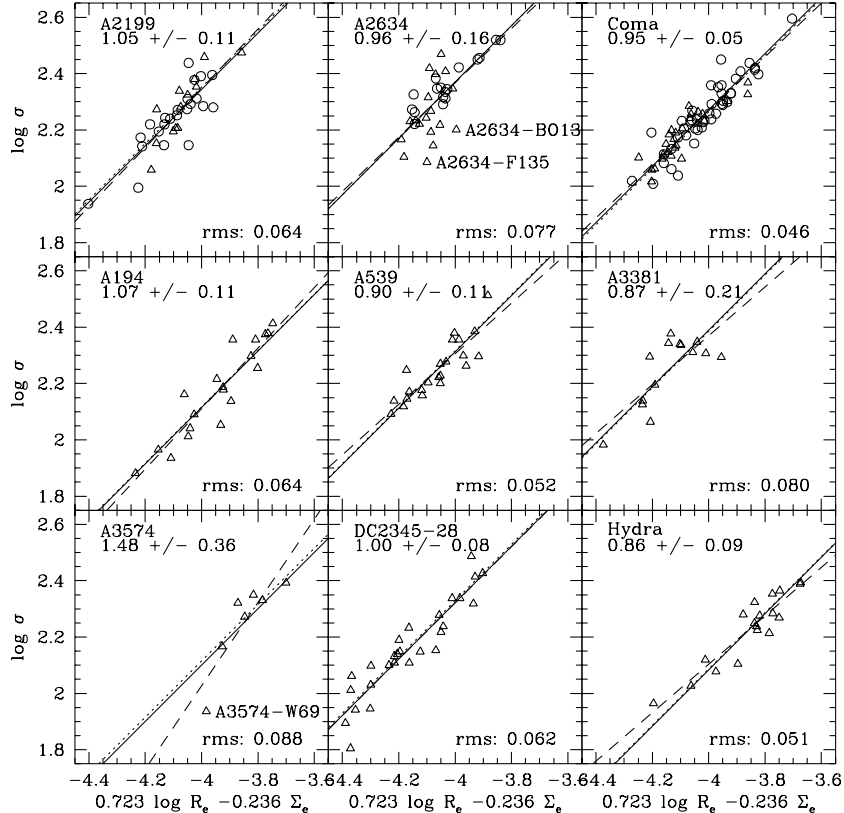


Fig. 3. FP data and fits for the calibration clusters A2199, A2634, Coma, A0194, A0539, A3381, A3574, DC2345-28 and Hydra. Symbols are as in Figure 2 for Coma, A2199 and A2634. For other clusters, all galaxies are indicated by triangles, irrespective of type. Lines are as in Figure 2

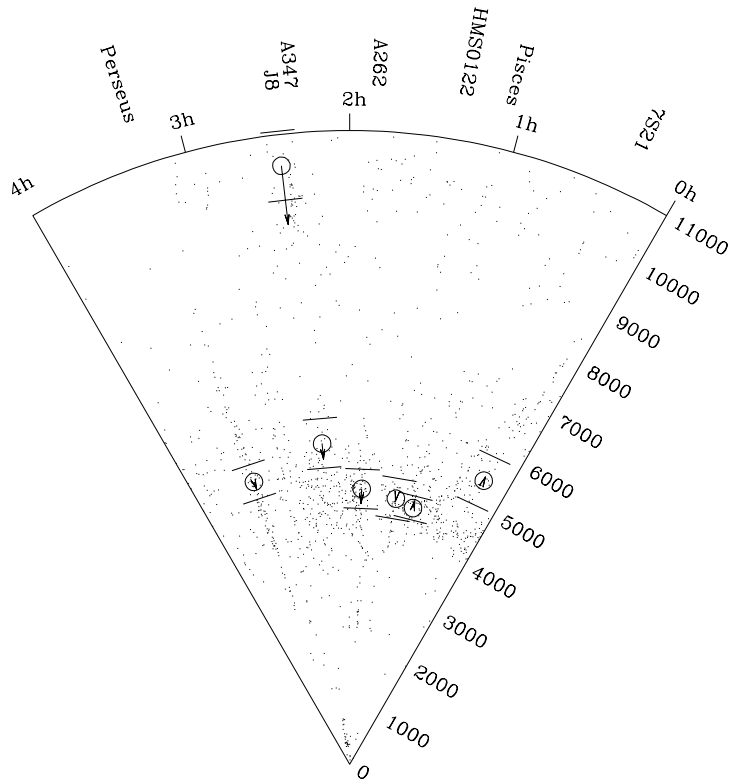


Fig. 4. Cone diagram showing peculiar velocity vectors deduced from this study. Small points indicate the CMB-frame redshift-space positions of galaxies from the ZCAT compilation (Huchra et al. 1993). PP clusters are shown at their inferred distances by open circles, with vectors extending to their CMB-frame velocities to indicate peculiar motions. 1σ position errors are indicated by the bracketing lines. The six ridge clusters have peculiar motions indistinguishable from zero. In the background of the supercluster, J8 has a significant peculiar velocity, as does A2634 which lies just outside the range of this plot.